09,08

Cold blue phosphors based on dysprosium-doped aluminum oxide

© I.V. Baklanova, V.N. Krasil'nikov, A.P. Tyutyunnik, Ya.V. Baklanova

Institute of Solid State Chemistry, Russian Academy of Sciences,
Ural Branch, Yekaterinburg, Russia

E-mail: baklanova_i@ihim.uran.ru

Received August 30, 2021
Revised August 30, 2021
Accepted September 3, 2021

$Al_2O_3:Dy^{3+}$ oxides with different color luminescence were synthesized using precursor technology. The phase composition and crystal structure of the obtained materials were established by X-ray powder diffraction analysis. The excitation and emission spectra, decay curves, thermal quenching of luminescence were studied. Under UV-excitation, the phosphors exhibit blue, purplish blue, and white emission depending on the dysprosium concentration and the annealing temperature of the $Al_{1-x}Dy_x(OH)(HCOO)_2$ precursor in air.

Keywords: aluminum oxide, dysprosium, precursor synthesis method, luminescence, color coordinates.

DOI: 10.21883/PSS.2022.01.52494.196

1. Introduction

Luminescent materials with colored and white emission are being intensively studied due to the real prospect of use in the manufacture of light-emitting diodes, liquid-crystal and plasma displays, lighting fixtures, radiation dose meters etc., [1]. The great importance for the development of modern optical and digital technology is the creation of phosphors, which make it possible to adjust the color characteristics of emission and provide the required color scheme. One of the most frequently used methods for setting the radiation color is based on rational choice of luminescent hosts and impurity ions with overlapping emission spectra. In recent times, materials emitting blue or pale-blue light have become greatly important in the context of production of white-luminescence phosphors. Thus, a combination of blue luminescence of InGaN and yellow one of $YAG:Ce^{3+}$ made it possible, for the first time, to produce a commercial white light-emitting diode (WLED) [2]. Sources of blue emission, in addition to InGaN, can be, for instance, ZnS [3], AWO_4 ($A = Ca$, Sr, Ba) [4] and $NaYF_4$ [5] doped with Tm^{3+} ions, as well as $BaMgAl_{10}O_{17}$ doped with Eu^{2+} ions [6,7]. However, significant drawbacks of the described [2–7] luminescent materials were revealed during their operation. For instance, $InGaN/YAG:Ce^{3+}$ is characterized by a separation of the blue and yellow spectral ranges, as well as unsatisfactory color rendering due to absence of the red spectrum component. Blue $ZnS:Tm^{3+}$ phosphors are noted for a high light output, but are chemically unstable and apt to thermal quenching of luminescence at relatively low operating temperatures [3]. Thulium (III) doping of tungstates AWO_4 makes it possible to obtain blue emission under UV-excitation ($^1D_2 \rightarrow {}^3F_4$ electronic transition in the Tm^{3+} ion), but due to small absorption it is very weak in the visible spectrum range [4]. Efficiency of luminescence of Tm^{3+} ions in a $NaYF_4$ host can be increased by energy transfer from other ions, e.g., Ce^{3+}, Eu^{2+} or Dy^{3+} [5]. Despite the high intensity of blue luminescence, $BaMgAl_{10}O_{17}:Eu^{2+}$ is apt to oxidative breakdown during operation, which is related to the oxidation of Eu^{2+} ions to Eu^{3+}, gradually leading to a decrease of its luminescent characteristics [8]. Moreover, the excitation spectrum demonstrate that $BaMgAl_{10}O_{17}:Eu^{2+}$ has strong absorption in the short-wave and medium-wave UV-range and much lower absorption in the long-wave range, which is absolutely unsuitable for light-emitting diode manufacture. Pale-blue luminescence hosts are known, e.g., $NaCaBO_3$ and $Gd_5Si_3O_{12}N$, activated by cerium (III) ions [9,10]. The substitution of expensive europium by relatively cheap cerium is commercially efficient, but the presence of cerium in luminescent materials, as in the case of Eu^{2+} [6,7], requires particular synthesis conditions that prevent transition of Ce^{3+} into Ce^{4+}. Taking this into account, a vital task is the search for and development of new cheaper phosphors of the blue spectrum with good emission characteristics and stable in the operation conditions, synthesis of which is based on simple process solutions. In the previous papers [11–13] we have showed that the nanodispersed aluminum oxide obtained by heat treatment of the basic aluminum formiate ($Al(OH)(HCOO)_2$) is characterized by blue emission with the maximum of about 450 nm, which originates due to the presence of intrinsic defects and/or carbon impurity. The nanodispersed oxides $Al_2O_3:Ln$ ($Ln = Eu^{3+}/Tb^{3+}$) with a dopant content of 2.5 mol% were synthesized by thermolysis of precursors $Al_{1-x}Ln_x(OH)(HCOO)_2$ in the air at 700°C [14]. The calculated color coordinates demonstrate that the luminescence color of these compounds is close to white [15]. The ionic radius of the Dy^{3+} ion is less than the radii of Eu^{3+} and Tb^{3+} ions (Dy^{3+}(VI) 0.912 Å) [16], while in the range of 400−760 nm it can demonstrate blue, yellow and red luminescence, related to $^4F_{9/2} \rightarrow {}^6H_{15/2}$, $^4F_{9/2} \rightarrow {}^6H_{13/2}$, $^4F_{9/2} \rightarrow {}^6H_{11/2}$ f–f-transitions. It is known that an electric

dipole transition $^4F_{9/2} \rightarrow {}^6H_{13/2}$ is particularly sensitive to the environment of the dysprosium ion in a host in contrast to the magnetic dipole transition $^4F_{9/2} \rightarrow {}^6H_{15/2}$ [17]. When a Dy^{3+} ion takes up low-symmetrical positions in a host, the yellow emission is more dominating as compared to blue emission. On the contrary, blue emission will prevail when Dy^{3+} ions are in high-symmetrical sites. All these structural features eventually affect the total color emission of phosphors. The study of the emission of $Al_2O_3:Dy^{3+}$ has already been presented in some papers [18–22], but none of them informs of the contribution of the aluminum oxide host to luminescence in the visible range. The publications mainly concern the selection of an optimal activator content in the α-Al_2O_3 host, which does not cause concentration quenching of luminescence. This paper presents the structural, optical and luminescent characteristics of $Al_2O_3:Dy^{3+}$ powders obtained by annealing of precursor in the air, as well as establishes the influence of dysprosium concentration and the heat treatment conditions for the $Al_{1-x}Dy_x(OH)(HCOO)_2$ precursor on luminophore emission color of phosphors. The possibility of dosed substitution of aluminum by lanthanide in the precursor, and, respectively, in the synthesized aluminum oxide is an important advantage of the used precursor technology.

2. Experimental procedure

To obtain dysprosium-doped aluminum oxide $Al_2O_3:Dy^{3+}$, a precursor synthesis procedure was developed, which includes the preparation of the oxide by heating of the $Al_{1-x}Dy_x(OH)(HCOO)_2$ precursor in air. $Al_{1-x}Dy_x(OH)(HCOO)_2$ with $x = 0.005$, 0.01, 0.02 and 0.025 was synthesized by the following reaction:

$$(2-2x)Al(NO_3)_3 + 2xDy(NO_3)_3 + 19HCOOH = 2Al_{1-x}Dy_x(OH)(HCOO)_2 + 3N_2 + 15CO_2 + 16H_2O. \quad (1)$$

Analytically pure aluminum nitrate $Al(NO_3)_3 \cdot 9H_2O$, dysprosium nitrate $Dy(NO_3)_3 \cdot 6H_2O$ and formic acid (99.7% HCOOH) were used as reagents, distilled water was used as a solvent. Aluminum nitrate and dysprosium nitrate, taken in stoichiometric amounts according to the chemical formula $Al_{1-x}Dy_x(OH)(HCOO)_2$, were dissolved in diluted formic acid (20%) at room temperature. The solution was evaporated at 60°C to dry residue in the form of white powder, and ground in a porcelain mortar. To obtain oxides, $Al_{1-x}Dy_x(OH)(HCOO)_2$ precursors were heated at 700, 900 and 1100°C in air for 2 hours. X-ray powder diffraction (XRPD) analysis of the synthesized samples was performed using a STADI-P (STOE) diffractometer equipped with a linear position-sensitive detector. Recording X-ray patterns was performed in $CuK_{\alpha 1}$ radiation in the 2θ ranges from 5 to 120° with the step of 0.02°. Polycrystalline silicon ($a = 5.43075(5)$ Å) was used as an external standard.. The phases were identified using the PDF2 database (ICDD, 2016). The crystal structures of compounds were clarified by the method of full-profile Rietveld analysis using the GSAS software package [23,24]. The Raman spectrum was recorded at room temperature using a confocal Raman microscope Renishaw InVia Reflex ($\lambda = 532$ nm, $P = 5$ mW). Thermal analysis was performed on Netzsch STA 449 F3 Jupiter thermoanalyzer in air at the heating rate of 10°/min. Excitation and emission spectra, decay curves were recorded using a Varian Cary Eclipse fluorimeter (Xe lamp). Luminescence spectra in the temperature range of 25 to 150°C were recorded using a temperature cell holder GS-21525 (Specac Ltd).

3. Experimental results and discussion

As has been shown by the example of $Al_{1-x}Dy_x(OH)(HCOO)_2$ with the dysprosium content of 2 mol./% ($x = 0.02$), the precursors, synthesized by the reaction (1) are structurally identical to aluminum hydroxoformiate $Al(OH)(HCOO)_2$ [25]. The diffraction pattern of $Al_{0.98}Dy_{0.02}(OH)(HCOO)_2$ (Fig. 1) was indexed in a monoclinic system (space group $C2$) with the unit cell parameters: $a = 8.900(2)$ Å, $b = 9.955(3)$ Å, $c = 10.262(2)$ Å, $\beta = 106.41(1)°$, $V = 872.2(4)$ Å^3.

The formation of dysprosium-substituted hydroxoformiate $Al_{1-x}Dy_x(OH)(HCOO)_2$ with a structure of $Al(OH)(HCOO)_2$ is confirmed by Raman-spectroscopy data (Fig. 2) [13,14,25]. The frequency of 1068 cm^{-1} is responsible for out-of-plane bending vibrations of the C−H bond. Stretching vibrations of C−H bonds are recorded at 2922, 2937, 2978, and 3015 cm^{-1}. The line at 784 cm^{-1} corresponds to scissor vibrations of COO−. The frequencies of 1653 and 1552 cm^{-1} (ν_{as}(COO−)), 1412 and 1392 cm^{-1} (ν_s(COO−)) belong to asymmetric and symmetric stretching vibrations of the carboxylate-ion, respectively. The low-intensity line at 3489 cm^{-1} is related

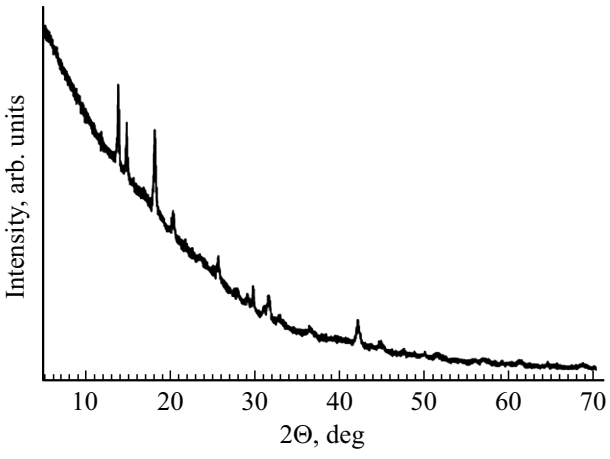

Figure 1. X-ray powder diffraction patterns of $Al_{0.98}Dy_{0.02}(OH)(HCOO)_2$.

to stretching vibrations of O−H bonds of metal-coordinated hydroxide-ions. Lines below 500 cm^{-1} refer to stretching vibrations of Al(Dy)−O bonds.

Thermogravimetric analysis was performed for the $Al_{0.99}Dy_{0.01}(OH)(HCOO)_2$ precursor (Fig. 3). The precursor decomposes when heated to 700°C in two main stages with the total weight loss of 61.44%, which corresponds to the weight loss (61.33%) upon the formation of oxide $(Al_{0.99}Dy_{0.01})_2O_3$. The small weight loss ($\sim 6\%$), observed at the first stage (up to 291°C), is caused by water removal due to thermally-stimulated decomposition of OH-groups and formation of a hypothetical phase $(Al_{0.99}Dy_{0.01})_2O(HCOO)_4$, similar to $Al_2O(HCOO)_4$ [26]. The second decomposition stage is characterized by a narrow temperature interval ($\sim 300-350$°C) and a greater weight loss ($\sim 55.5\%$), related to the decomposition of the organic component $(Al_{0.99}Dy_{0.01})_2O(HCOO)_4$ and release of gaseous products. The slight weight loss ($\sim 0.5\%$), observed on the TG curve, in the temperature interval of $\sim 350-500$°C is probably due to the removal of elemental carbon that forms precursor thermolysis of precursor [11].

In order to synthesize $(Al_{1-x}Dy_x)_2O_3$ samples, the $Al_{1-x}Dy_x(OH)(HCOO)_2$ precursors with $x = 0.005$, 0.01, 0.02 and 0.025 were heated at 700, 900 and 1100°C in air, with holding for 2 h at each temperature. According to the XRPD data, the oxide samples obtained by heating of precursor at 700°C are X-ray amorphous. Figure 4 demonstrates the diffraction patterns for the samples $(Al_{1-x}Dy_x)_2O_3$ ($x = 0.005$, 0.01 and 0.02), obtained at 900°C, which have γ-Al_2O_3 structure (space group $I4_1/amd$, #141) (Table 1). The sample with $x = 0.025$, in addition to γ-$(Al_{1-x}Dy_x)_2O_3$ (98.5 mass%), has a small contents of impurity phases of $DyAlO_3$ (0.6 mass%) and $Dy_3Al_5O_{12}$ (0.9 mass%). The samples obtained by precursor annealing at the temperature of 1100°C are also mixed-phase. For instance, the sample with $x = 0.005$, in addition to a phase with the γ-Al_2O_3 structure, contains an α-modification of Al_2O_3 (10.1 mass%), whereas the sample with $x = 0.02$ also comprises small amounts of $DyAlO_3$ (1.1 mass%). Thus, the annealing of $Al_{1-x}Dy_x(OH)(HCOO)_2$ precursors, with $0.005 \le x \le 0.02$ at the temperature of 900°C results in the formation of solid solutions $(Al_{1-x}Dy_x)_2O_3$ the γ-Al_2O_3 structure. Upon heating to 1100°C, the oxide with the γ-Al_2O_3 structure partially transforms into an oxide with the α-Al_2O_3 structure. We have shown earlier that, as a result of $Al(OH)(HCOO)_2$ heating in air, γ-Al_2O_3 forms already at 750°C, while its transformation into α-Al_2O_3

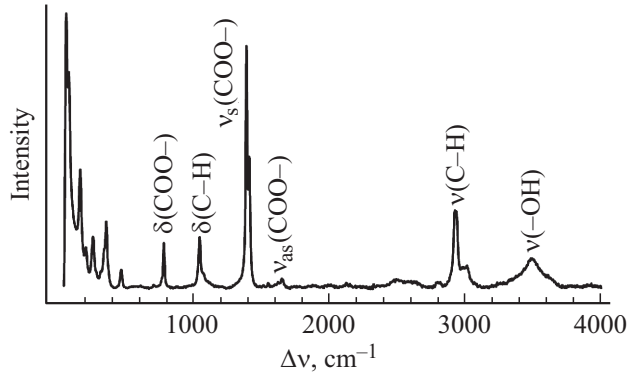

Figure 2. Raman spectrum of $Al_{0.98}Dy_{0.02}(OH)(HCOO)_2$.

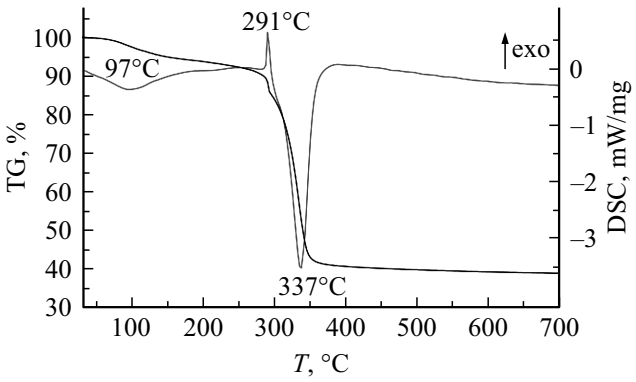

Figure 3. TG and DSC curves for $Al_{0.99}Dy_{0.01}(OH)(HCOO)_2$.

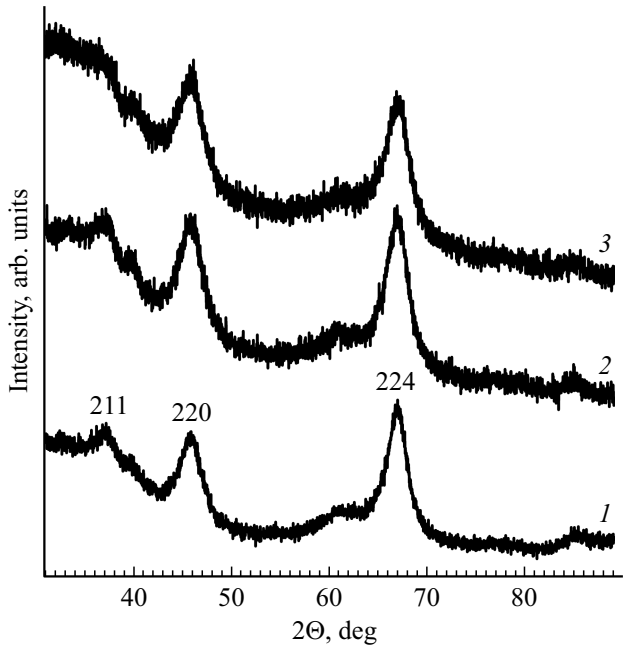

Figure 4. X-ray powder diffraction patterns of γ-$(Al_{1-x}Dy_x)_2O_3$: $x = 0.005$ (*1*), 0.01 (*2*) and 0.02 (*3*).

Table 1. Lattice parameters for $(Al_{1-x}Dy_x)_2O_3$, obtained by heating of $Al_{1-x}Dy_x(OH)(HCOO)_2$ precursors 900°C in air

x	0.005	0.01	0.02
a, Å	5.594(2)	5.636(2)	5.642(2)
c, Å	7.912(3)	7.962(3)	7.978(3)
V, Å^3	247.6(1)	252.9(1)	253.9(1)

begins at 950°C [11]. Consequently, doping with Dy^{3+} ions significantly affects the structure of the aluminum oxide host, causing an increase in the temperature of phase transition $\gamma \rightarrow \alpha$ [14]. Aluminum atoms in the γ-Al_2O_3 oxide with the spinel structure $\square_{2(2/3)}Al_{21(1/3)}O_{32}$ ($\square$ = Al vacancies) are in an octahedral and tetrahedral environment [26]. In the structure of defective spinel γ-Al_2O_3, cation vacancies occupy octahedral sites [27–29]. Dy^{3+} ions do not have a coordination number lower than six, therefore they can substitute aluminum (Al^{3+}(VI) 0.535 Å [16]) only in octahedral sites in γ-Al_2O_3 [14].

In our previous papers, we have already shown that the heat treatment method for the $Al(OH)(HCOO)_2$ precursor considerably affects the emission characteristics of oxides [11–14]. Aluminum oxide, obtained by thermolysis of the $Al(OH)(HCOO)_2$ precursor in air, demonstrates blue luminescence with the maximum of $\sim$ 450 nm, which appears due to intrinsic defects of the aluminum oxide and/or precursor carbon residue. Figure 5 shows the excitation spectrum of γ-$(Al_{0.995}Dy_{0.005})_2O_3$ under Decay 572 nm wavelength. The narrow lines refer to electronic transitions from the ground level $^6H_{15/2}$ to higher energy levels of the Dy^{3+} ion: $^4F_{3/2}$ (295 nm), $^6P_{3/2}$ (325 nm), $^6P_{7/2}$ (350 nm), $^6P_{5/2}$ (365 nm), $^4I_{13/2}$ (386 nm), $^4F_{7/2}$ (426 nm) and $^4I_{15/2}$ (457 nm), respectively. The most intensive line is observed at 350 nm and corresponds to the $^6H_{15/2} \rightarrow {}^6P_{7/2}$ transition. The emission spectra for all the obtained samples upon UV-excitation (λ = 350 nm) consist of wide bands with the maximum in the blue region of the spectrum; these bands are superposition of the emission lines associated with intrinsic defects of the host and f–f transitions in Dy^{3+} ions (Fig. 5). The spectrum shows the superposition luminescence lines that refer to f–f-transitions in Dy^{3+} ion: $^4G_{11/2} \rightarrow {}^6H_{15/2}$ (445 nm), $^4I_{15/2} \rightarrow {}^6H_{15/2}$ (458 nm), $^4F_{9/2} \rightarrow {}^6H_{15/2}$ (477 nm), $^4F_{9/2} \rightarrow {}^6H_{13/2}$ (572 nm), $^4F_{9/2} \rightarrow {}^6H_{11/2}$ (681 nm), $^4F_{9/2} \rightarrow {}^6H_{9/2} + {}^6F_{11/2}$ (699 nm), $^4F_{9/2} \rightarrow {}^6H_{7/2} + {}^6F_{9/2}$ (764 nm). One can note a considerable change in luminescence intensity depending on dysprosium concentration and annealing temperature of precursor (Fig. 5). As the precursor annealing temperature increases, emission intensity decreases and quenching of luminescence of the aluminum oxide host is observed. A similar dependence of luminescence intensity on annealing temperature of precursor was observed for the products of the thermolysis of $Al(OH)(HCOO)_2$ obtained in air and in helium and is related to structural changes in the aluminum oxide host [11]. Dysprosium doping of aluminum oxide also suppresses the blue luminescence. However, if we trace the change in intensity of the lines that refer to dysprosium ion transitions, we can note that luminescence quenching is observed only for the sample obtained by thermolysis of the $Al_{0.98}Dy_{0.02}(OH)(HCOO)_2$ precursor at 1100°C. As dysprosium concentration increases, distance between activator ions becomes smaller, leading to a higher probability of nonradiative energy transfer. The aluminum oxide sample obtained at 1100°C contains impurity phases (α-Al_2O_3 and $DyAlO_3$) which may also affect the luminescence quenching. For the other samples, the line intensities, referred to transitions $^4F_{9/2} \rightarrow {}^6H_{13/2}$ (572 nm), $^4F_{9/2} \rightarrow {}^6H_{11/2}$ (681 nm), $^4F_{9/2} \rightarrow {}^6H_{9/2} + {}^6F_{11/2}$ (699 nm), $^4F_{9/2} \rightarrow {}^6H_{7/2} + {}^6F_{9/2}$ (764 nm) do not strongly depend on dysprosium concentration. There is also no Shift of the intensity maxima towards a longer or shorter wavelengths with a change in Dy^{3+} ion concentration is also absent.

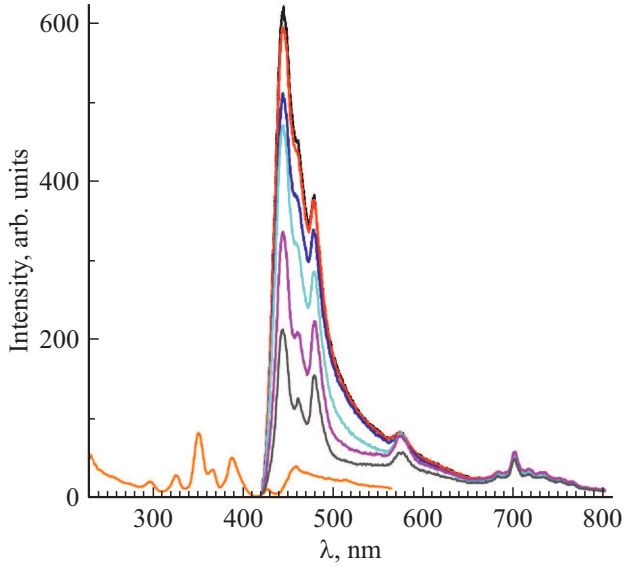

Figure 5. Excitation spectrum (λ = 573 nm (orange) and emission spectra (λ = 350 nm) for the products of the thermolysis of $Al_{1-x}Dy_x(OH)(HCOO)_2$ precursors at various annealing temperatures in air: x = 0.005 at 700°C (black), x = 0.005 at 900°C (red), x = 0.005 at 1100°C (darkblue), x = 0.02 at 700°C (blue), x = 0.02 at 900°C (pink) and x = 0.02 at 1100°C (grey).

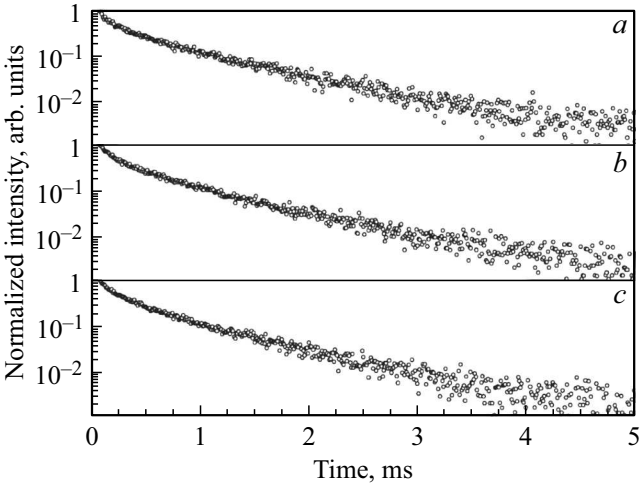

Figure 6. Decay curves for the products of the thermolysis of $Al_{1-x}Dy_x(OH)(HCOO)_2$ precursors at x = 0.005 (a), x = 0.01 (b) and x = 0.02 (c), measured at λ_{ex} = 350 nm and λ_{em} = 479 nm.

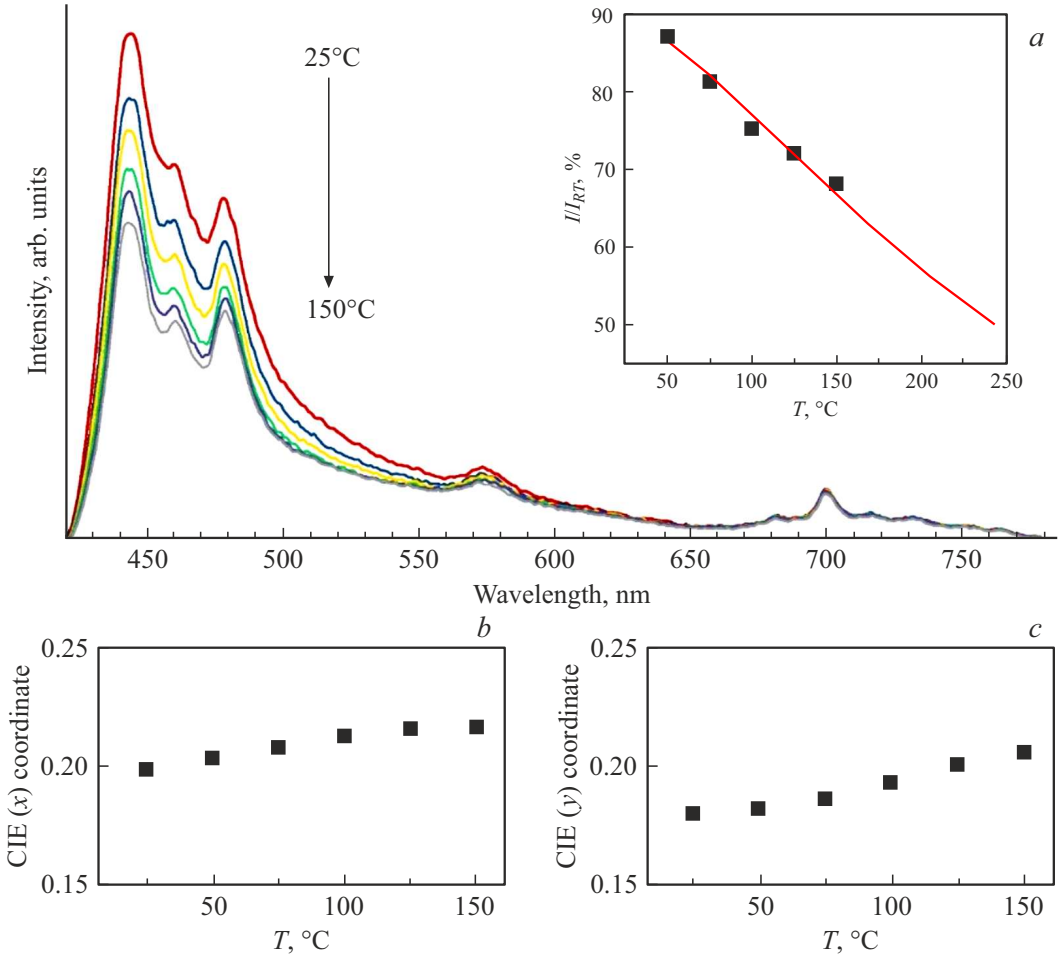

Figure 7. Luminescence spectra ($\lambda_{ex} = 350$ nm) for the products of the thermolysis of $Al_{0.995}Dy_{0.005}(OH)(HCOO)_2$, measured at different heating temperatures (a); temperature dependences of integral luminescence intensity (the insert) and values of color coordinates (x, y) (b, c).

The decay curves (Fig. 6) for γ-$(Al_{1-x}Dy_x)_2O_3$ with $x = 0.005$, 0.01 and 0.02 were recorded under excitation at 350 nm by monitoring the emission at 479 nm and can be approximated by a double exponential function. The calculated average lifetimes for γ-$(Al_{1-x}Dy_x)_2O_3$ are equal to 0.6 ms ($x = 0.005$), 0.52 ms ($x = 0.01$) and 0.51 ms ($x = 0.02$), and are close to the values obtained for different dysprosium-doped compounds [30–32]. The double exponential profile of decay curves, as well as lifetime decrease with dysprosium concentration can be explained both by energy transfer from the aluminum host to Dy^{3+} ions, processes of cross-relaxation between neighboring Dy^{3+} ions and by inhomogeneous distribution of luminescent centers in the aluminum host [30,31].

The parameters under excitation at 350 nm by monitoring the emission at 479 nm characterizing the emission color of the studied compounds were calculated from the luminescence spectra under 350 nm excitation and are given in Table 2. Chromaticity coordinates (x, y) for the phosphor obtained by heating of $Al_{0.98}Dy_{0.02}(OH)(HCOO)_2$ precursor at 1100°C, are (0.24, 0.22) and are located on the diagram suggested by K.L. Kelly in the white color region [15]. Sample color purity, calculated according to the chromaticity coordinates of a white color source and the dominant wavelength ($\lambda = 443$ nm [33]), varies from ~ 60 to $\sim 40\%$ (Table 2).

A significant change in emission of phosphor with temperature rise casts doubts on its technological prospects, therefore estimation of thermal stability is one of the mandatory characteristics in the study of new emitting materials. The maintaining of sufficient emission efficiency at temperatures above 150°C [34] is acceptable for compounds considered for use in the visible spectral range. Accordingly, the temperature (thermal quenching temperature — $T_{50\%}$), at which a compound demonstrates half of its emission intensity registered at room temperature, is a threshold value that determines the future prospects of phosphor. The luminescence spectra ($\lambda_{ex} = 350$ nm) for the γ-$(Al_{0.995}Dy_{0.005})_2O_3$ compound, measured in a wide temperature range, are given in Fig. 7. Gradual sample heating to 150°C is accompanied with a decrease in intensity of emission lines in the blue spectral range,

Table 2. Color coordinates (x, y) for the products of the thermolysis of $Al_{1-x}Dy_x(OH)(HCOO)_2$ precursors at various temperatures in air

x	T, °C	x	y	Emission color	Color purity, %
0.005	700	0.19	0.17	blue	59.31
	900	0.19	0.17	blue	59.31
	1100	0.20	0.18	blue	55.37
0.02	700	0.20	0.17	purplish blue	57.51
	900	0.23	0.18	purplish blue	50.29
	1100	0.24	0.22	white	39.65

which are related to intrinsic defects of the aluminum oxide host, while intensity of emission line in the long-wave range corresponding to f–f transitions in dysprosium ions remains almost unchanged. When powder is heated to 150°C, luminescence intensity is 68% of the initial value. The calculated dependence $I/I_{RT} = f(T)$, showed in the insert for Fig. 7 is described by a modified Arrhenius equation [35], and makes it possible to accurately determine the thermal quenching temperature. The compound demonstrates a high thermal stability of emission: the calculated value of $T_{50\%}$ is 245°C, while chromaticity coordinates remain unchanged in the whole recorded temperature range (Fig. 7).

4. Conclusion

Phosphors based on dysprosium-doped aluminum oxide $Al_2O_3:Dy^{3+}$ have been obtained by thermal decomposition of $Al_{1-x}Dy_x(OH)(HCOO)_2$ precursors in air. Analysis of the structural data shows that oxides γ-$(Al_{1-x}Dy_x)_2O_3$ ($x = 0.005$, 0.01, 0.02) form during thermolysis of precursors only at the temperature of 900°C. The broad and intensive luminescence of synthesized samples in the visible range with maxima in the blue region is due to the overlapping of the emission lines caused by internal defects of the Al_2O_3 host and f–f transitions in the Dy3+ ion. the Dy^{3+} ion. According to the color coordinates, the synthesized oxides have different color emission depending on dysprosium concentration and annealing temperature of precursor. Given the high thermal stability of emission, $Al_2O_3:Dy^{3+}$ oxides become very attractive compounds for use as cold-light phosphors.

Funding

The work has been carried out in accordance with the state assignment for the Institute of Solid State Chemistry of the Ural Branch of the Russian Academy of Sciences and scientific plans in the field of fundamental scientific research (No. AAAA-A19-119031890025-9).

Conflict of interest

The authors declare that they have no conflict of interest.

References

[1] G.B. Nair, H.C. Swart, S.J. Dhoble. Prog. Mater. Sci. **109**, 100622 (2020).
[2] S. Nakamura. J. Vac. Sci. Technol. A **13**, 705 (1995).
[3] D. Adachi, H. Haze, H. Shirahase, T. Toyama, H. Okamoto. J. Non-Cryst. Solids **352**, 1628 (2006).
[4] J. Liao, B. Qiu, H. Wen, J. Chen, W. You, L. Liu. J. Alloys Compd. **487**, 758 (2009).
[5] V.N.K.B. Adusumalli, S. Sarkar, V. Mahalingam. Chem. Phys. Chem. **16**, 2312 (2015).
[6] K.B. Kim, Y.I. Kim, H.G. Chun, T.Y. Cho, J.S. Jung, J.G. Kang. Chem. Mater. **14**, 5045 (2002).
[7] L. Ye, X. Peng, S. Zhang, Y. Wang, W. Chang. J. Rare Earths **32**, 1109 (2014).
[8] P. Boolchand, K.C. Mishra, M. Raukas, A. Ellens, P.C. Schmidt. Phys. Rev. B **66**, 134429 (2002).
[9] X. Zhang, J. Song, C. Zhou, L. Zhou, M. Gong. J. Lumin. **149**, 69 (2014).
[10] F. Lu, L. Bai, Z. Yang, X. Han. Mater. Lett. **151**, 9 (2015).
[11] V.N. Krasil'nikov, I.V. Baklanova, V.P. Zhukov, N.I. Medvedeva, A.P. Tyutyunnik, R.F. Samigullina, O.I. Gyrdasova, M.A. Melkozerova. J. Alloys Compd. **698**, 1102 (2017).
[12] M.A. Melkozerova, O.I. Gyrdasova, I.V. Baklanova, E.V. Vladimirova, E.V. Zabolotskaya, V.N. Krasil'nikov. Mendeleev Commun. **28**, 668 (2018).
[13] I.V. Baklanova, V.N. Krasil'nikov, A.P. Tyutyunnik, A.N. Enyashin, Ya.V. Baklanova, O.I. Gyrdasova, R.F. Samigullina, E.G. Vovkotrub. Spectrochim. Acta A **227**, 117658 (2020).
[14] I.V. Baklanova, V.N. Krasil'nikov, A.P. Tyutyunnik, Ya.V. Baklanova. J. Solid State Chem. **292**, 121699 (2020).
[15] K.L. Kelly. J. Opt. Soc. Am. **33**, 627 (1943).
[16] R.D. Shannon. Acta Cryst. A, **32**, 751 (1976).
[17] G.B. Nair, S.J. Dhoble. RSC Adv. **5**, 49235 (2015).
[18] T. Ishizaka, Y. Kurokawa. J. Lumin. **92**, 57 (2001).
[19] S. Kumar, R. Prakash, V. Kumar. Funct. Mater. Lett. **8**, 1550061 (2015).
[20] N. Ishiwada, E. Fujii, T. Yokomori. J. Lumin. **196**, 492 (2018).
[21] R. Martínez-Martínez, S. Rivera, E. Yescas-Mendoza, E. Álvarez, C. Falcony, U. Caldiño. Opt. Mater. **33**, 1320 (2011).
[22] S. Stojadinović, A. Cirić. J. Lumin. **226**, 117403 (2020).
[23] B.H. Toby. J. Appl. Crystallogr. **34**, 210 (2001).
[24] A.C. Larson, R.B. Von Dreele. General Structure Analysis System (GSAS). Los Alamos, NM (2004). Los Alamos National Laboratory Report LAUR 86–748.
[25] V.N. Krasil'nikov, A.P. Tyutyunnik, I.V. Baklanova, A.N. Enyashin, I.F. Berger, V.G. Zubkov. CrystEngComm. **20**, 2741 (2018).
[26] K. Sohlberg, S.J. Pennycook, S.T. Pantelides. J. Am. Chem. Soc. **121**, 7493 (1999).
[27] J.M.A. Caiut, L. Bazin, R. Mauricot, H. Dexpert, S.J.L. Ribeiro, J. Dexpert-Ghys. J. Non-Cryst. Solids **354**, 4860 (2008).
[28] A. Rastorguev, M. Baronskiy, A. Zhuzhgov, A. Kostyukov, O. Krivoruchko, V. Snytnikov. RSC Adv. **5**, 5686 (2015).
[29] G. Gutierrez, A. Taga, B. Johansson. Phys. Rev. B **65**, 012101 (2001).

[30] J. Zhang, Q.Guo, L. Liao, Y. Wang, M. He, H. Ye, L. Mei, H. Liu, T. Zhou, B. Ma. RSC Adv. **8**, 38883 (2018).
[31] Z. An, X. Xiao, J. Yu, D. Mao, G. Lu. RSC Adv. **5**, 52533 (2015).
[32] U. Fawad, H.J. Kim, S. Khan, M. Khan, L. Ali. Solid State Sci. **62**, 1 (2016).
[33] J.S. Kumar, K. Pavani, A.M. Babu, N.K. Giri, S.B. Rai, L.R. Moorthy. J. Lumin., **130**, 1916 (2010).
[34] J. Li, J. Yan, D. Wen, W. Ullah Khan, J. Shi, M. Wu, Q. Su, P.A. Tanner. J. Mater. Chem. C **4**, 8611, (2016).
[35] V. Bachmann, C. Ronda, O. Oeckler, W. Schnick, A. Meijerink. Chem. Mater. **21**, 316 (2009).